



Universiteit  
Leiden  
The Netherlands

## **Cross-linkable polyion complex micelles from polypept(o)ide-based ABC-triblock copolymers for siRNA delivery**

Capelôa, L.; Yazdi, M.; Zhang, H.; Chen, X.; Nie, Y.; Wagner, E.; ... ; Barz, M.

### **Citation**

Capelôa, L., Yazdi, M., Zhang, H., Chen, X., Nie, Y., Wagner, E., ... Barz, M. (2021). Cross-linkable polyion complex micelles from polypept(o)ide-based ABC-triblock copolymers for siRNA delivery. *Macromolecular Rapid Communications*, 43(12).  
doi:10.1002/marc.202100698

Version: Publisher's Version

License: [Creative Commons CC BY-NC 4.0 license](#)

Downloaded from: <https://hdl.handle.net/1887/3250337>

**Note:** To cite this publication please use the final published version (if applicable).

# Cross-Linkable Polyion Complex Micelles from Polypept(o)ide-Based ABC-Triblock Copolymers for siRNA Delivery

Leon Capelôa, Mina Yazdi, Heyang Zhang, Xiaobing Chen, Yu Nie, Ernst Wagner, Ulrich Lächelt, and Matthias Barz\*

ABC-type triblock copolymers are a rising platform especially for oligonucleotide delivery as they offer an additional functionality besides the anyhow needed functions of shielding and complexation. The authors present a polypept(o)ide-based triblock copolymer synthesized by amine-initiated ring-opening polymerization (ROP) of *N*-carboxyanhydrides (NCAs), comprising a shielding block A of polysarcosine (pSar), a poly(*S*-ethylsulfonyl-L-cystein) (pCys(SO<sub>2</sub>Et)) block B for bioreversible and chemo-selective cross-linking and a poly(L-lysine) (pLys) block C for complexation to construct polyion complex (PIC) micelles as vehicle for small interfering RNA (siRNA) delivery. The self-assembly behavior of ABC-type triblocks is investigated to derive correlations between block lengths of the polymer and PIC micelle structure, showing an enormous effect of the  $\beta$ -sheet forming pCys(SO<sub>2</sub>Et) block. Moreover, the block enables the introduction of disulfide cross-links by reaction with multifunctional thiols to increase stability against dilution. The right content of the additional block leads to well-defined cross-linked 50–60 nm PIC micelles purified from production impurities and determinable siRNA loading. These PIC micelles can deliver functional siRNA into Neuro2A and KB cells evaluated by cellular uptake and specific gene knockdown assays.

## 1. Introduction

To follow the increasing interest in therapeutic nucleic acid delivery, a variety of delivery strategies such as lipid-based carriers, polymer-conjugates or nucleotide-derived nanoparticles have been developed and optimized over the past decades.<sup>[1]</sup> The concept of utilizing interaction between counter-charged polymers to form PIC micelles and their potential as delivery systems for oligonucleotides has already arisen in the late 90s.<sup>[2–4]</sup> Combining the cargo-protective core-shell structure of micelles with the ability to complex polyanions like DNA, RNA, and even proteins in the core, PIC micelles display a promising platform for current development.<sup>[5,6]</sup> However, to reach tissues that are not directly accessible, systemic applications are inevitable, facing well-known post-injection hurdles like aggregation or dilution by interaction with charged proteins in the blood, cargo degradation by nucleases, or immunological reactions by leaking oligonucleotides.<sup>[7]</sup> In order to bypass these adverse effects,

L. Capelôa, M. Barz  
Leiden Academic Centre for Drug Research (LACDR)  
Leiden University  
Einstein weg 55, Leiden 2333CC, The Netherlands  
E-mail: m.barz@lacdr.leidenuniv.nl


L. Capelôa, M. Barz  
Department of Dermatology  
University Medical Center  
Johannes Gutenberg-University Mainz  
Obere Zahlbacher Straße 63, 55131 Mainz, Germany

M. Yazdi, E. Wagner  
Pharmaceutical Biotechnology  
Department of Pharmacy  
LMU Munich  
Butenandtstrasse 5-13, 81377 Munich, Germany

H. Zhang  
Leiden Academic Center for Drug Research (LACDR)  
Leiden University  
Einstein weg 55, Leiden 2333CC, The Netherlands

X. Chen, Y. Nie  
National Engineering Research Center for Biomaterials  
Sichuan University  
Chengdu 610064, P. R. China

U. Lächelt  
Division of Pharmaceutical Technology and Biopharmaceutics  
University of Vienna  
Althanstrasse 14, Vienna 1090, Austria

 The ORCID identification number(s) for the author(s) of this article can be found under <https://doi.org/10.1002/marc.202100698>

© 2022 The Authors. Macromolecular Rapid Communications published by Wiley-VCH GmbH. This is an open access article under the terms of the Creative Commons Attribution-NonCommercial License, which permits use, distribution and reproduction in any medium, provided the original work is properly cited and is not used for commercial purposes.

DOI: 10.1002/marc.202100698

carrier systems can be intrinsically stabilized to keep structural integrity until reaching the site of action.<sup>[8,9]</sup> In this respect, the most common techniques are hydrophobic stabilization<sup>[10,11]</sup> and bioreversible cross-linking (mostly disulfide-mediated).<sup>[12,13]</sup>

These three major tasks of PIC micelles, i) cargo shielding from the biological environment, ii) intrinsic stabilization, and (iii) complexing properties, can be accomplished by ABC triblock copolymers, where block A builds up the shielding and surrounding corona, block B and C display core functionalities.<sup>[14–18]</sup> Polypept(o)ides (polypeptoid-*block*-polypeptide copolymers) are a material class capable of fulfilling all these demands and are based on building blocks that are derived from endogenous amino acids. In particular, they are able to combine the multifunctionality and diversity of polypeptides with the stealth-effect mediated by the polypeptoid pSar.<sup>[19,20]</sup> Synthetically, the material is accessible by nucleophilic ROP of NCAs, which can provide good control over chain length, size distribution, and block sequence under optimized conditions.<sup>[21–24]</sup> pSar is currently one of the most promising alternatives for the gold-standard polyethylene glycol as shielding-material in nanomedicine with comparable solution properties,<sup>[25]</sup> lower immunogenicity,<sup>[26]</sup> leads to carriers with neglectable protein corona<sup>[27,28]</sup> and just presented great potential by incorporation into lipid formulations.<sup>[29–31]</sup> To build a multi-functional ABC structured triblock copolymer, we combined pSar as shielding domain with a pCys(SO<sub>2</sub>Et) block B for bioreversible and chemo-selective cross-linking.<sup>[32,33]</sup> Moreover, pCys(SO<sub>2</sub>Et) forms antiparallel  $\beta$ -sheets, influencing and guiding the self-assembly behavior.<sup>[34–38]</sup> Consequently, block C is obliged to comprise polycationic moiety for complexation and cellular internalization of the polyanionic oligonucleotide. Possessing polypeptidic nature poly(L-ornithine) (pOrn),<sup>[39]</sup> poly(L-arginine) (pArg),<sup>[40,41]</sup> but most commonly pLys<sup>[12,42–45]</sup> is utilized, as it is in this study.

We herein report on the synthesis, characterization, and application of a new ABC-type triblock copolymer pSar-*b*-pCys(SO<sub>2</sub>Et)-*b*-pLys. Incorporation of a pCys(SO<sub>2</sub>Et) segment into an oligonucleotide complexing triblock polymeric structure has not yet been achieved before and will prove to provide unique features for the resulting PIC micelles, including controlled self-assembly and disulfide-mediated intrinsic stability. We provide insights into the formation and properties of cross-linkable PIC micelles loaded with siRNA to be used as drug delivery system for specific knock-down of gene expression. This occurs by siRNA-mediated degradation of the targeted mRNA inside the cytosol, a mechanism called RNA interference (RNAi), which offers enormous flexibility to manipulate cellular processes by addressing different target genes and therefore offers great potential for the treatment of a variety of diseases.<sup>[46–49]</sup>

## 2. Results and Discussion

### 2.1. ABC-Triblock Copolymer Synthesis and Characterization

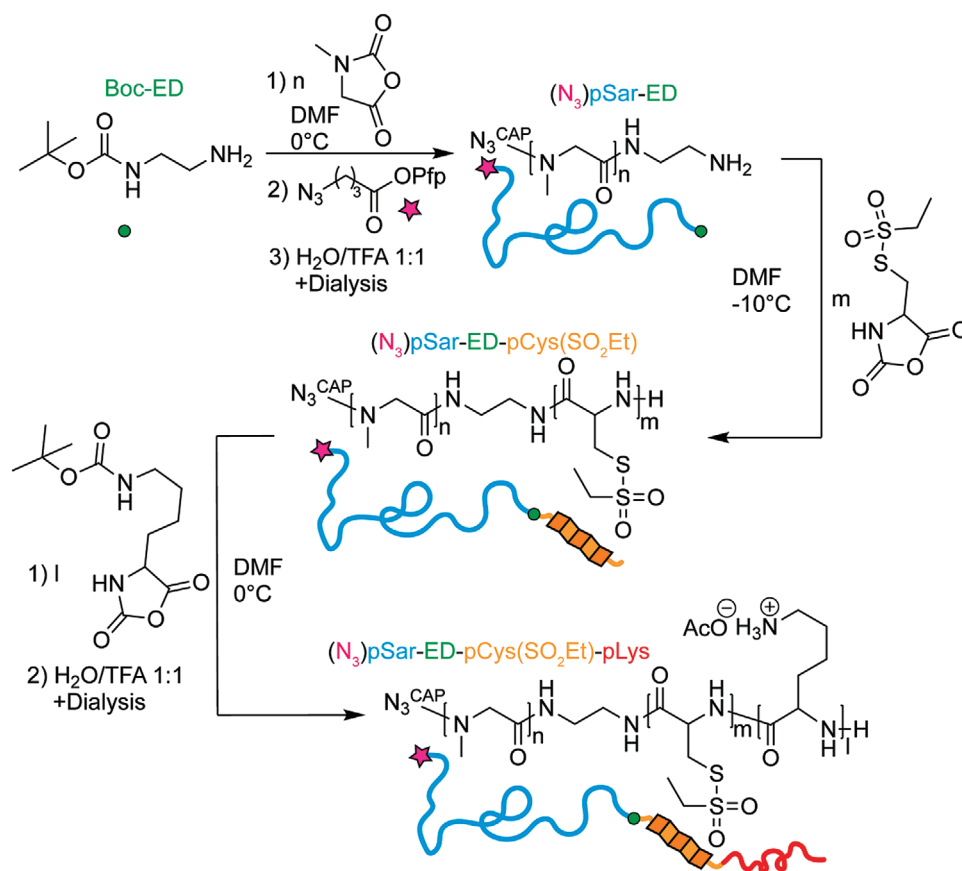
Amine-initiated ROP of the corresponding NCA gave access to controlled synthesis of the pSar-*b*-pCys(SO<sub>2</sub>Et)-*b*-pLys ABC-type triblock copolymer. Starting from the pSar block, a bi-functional initiator approach using *N*-(*tert*-butoxycarbonyl)-1,2-ethylenediamine (Boc-ED) was utilized, enabling introduction of an azide functionality by capping pSar reactive end group

and later outside of the carrier system while providing a primary amine functionality for further ROP of NCAs after Boc-deprotection (Figure S1, Supporting Information).<sup>[33]</sup> PCys(SO<sub>2</sub>Et) and pLys(Boc) as core-forming blocks B and C could then be polymerized sequentially from this primary amine-containing macroinitiator (**Scheme 1**). The complexing block C was introduced as pLys(Boc) since it offers acidic deprotection conditions to generate positive charges, avoiding the use of bases or the production of other soft nucleophiles, ensuring the stability of the *S*-ethylsulfonyl-protective group.<sup>[50]</sup>

Structural integrity is demonstrated in **Figure 1A** by <sup>1</sup>H diffusion-ordered (DOSY) NMR spectroscopy, showing all protons of the polymeric structure attributed to the only diffusing species besides solvent molecules. Gel permeation chromatography (GPC) in hexafluoro-2-propanol (HFIP) can further confirm narrow and monomodal size distribution ( $\bar{M}_w/\bar{M}_n = 1.40$ ), displaying controlled polymerization in the absence of side reactions producing homo- or diblock polymers (Figure 1B). Consistent chain growth is further visualized by the GPC elugram, represented by shifts to lower elution volumes. However, observed minor shifts can be explained by the ratio of repeating units, starting from a long pSar chain only growing a few repeat units of pCys(SO<sub>2</sub>Et) and pLys(Boc) upon chain extension. Chain length of the pSar block was determined by GPC elution volume relative to pSar-standards ( $X_{n,pSar} = 180$ ).<sup>[25]</sup> Normalizing on the pSar repeat units in NMR spectra of diblock and triblock copolymers, chain lengths of pCys(SO<sub>2</sub>Et) and pLys(Boc) were calculated with the isolated Cys- $\alpha$ H signal at 4.69 ppm ( $X_{n,pCys} = 9$ ) and the Lys-N<sub>H</sub>CO- signal at 6.56–6.76 ppm ( $X_{n,pLys} = 9$ ), respectively (Figures S2 and S3, Supporting Information). Complete Boc-deprotection of the pLys block can be confirmed by the absence of the characteristic amide- (6.56–6.76 ppm) and Boc-signal (1.37 ppm). Further, stability against deprotection conditions can be seen in HFIP GPC, where no degradation of the polymeric backbone is observed (Figures S4 and S5, Supporting Information). Minor changes in the elugram derive from altered interaction with the column material by free amines. The ratio of chain lengths 180/9/9 has been selected since this polymer forms monomodal size distributed PIC micelles. The effect of block sizes on aggregation will be discussed in the following section.

### 2.2. PIC Micelle Formation and Evaluation

With the successfully synthesized and characterized ABC-triblock copolymer, PIC micelle formation was investigated. In general, the literature describes formation of PIC micelles from unimolecular solved polymers interacting with the oligonucleotide (here: siRNA) by electrostatic attraction having the two major driving forces i) compensation of entropy loss by liberation of counterions and ii) aggregation into micelles by pseudo-amphiphilic structures deriving from charge neutralization of the polycationic block.<sup>[5,18,40,51,52]</sup> The PIC micelles can then be intrinsically stabilized by cross-linking of the core, in this case using triethylenetetramine dicysteine (cTETAc), as displayed in **Figure 2A**. The ability of the ABC-triblock copolymer to complex siRNA was confirmed by agarose gel electrophoresis (**Figure 2B**), showing the disappearance of the free siRNA band with increasing N/P-ratios. Prevented migration of free siRNA into the gel



**Scheme 1.** Synthetic route to derive  $(N_3)p\text{Sar-b-pCys(SO}_2\text{Et)-b-pLys}$  ABC-triblock copolymer from amine-initiated ROP of NCAs utilizing a bifunctional initiator approach followed by sequential polymerization and subsequent Boc-deprotection.

indicates formation of PIC micelles, that exhibit a larger size and therefore cannot penetrate through the gel pores. Consequently, staining of encapsulated siRNA is impeded. The N/P ratio of 5:1 was chosen for further experiments assuming complete siRNA encapsulation. Dynamic Light Scattering (DLS) confirmed PIC micelles with a z-average of 57.1 nm (Pdl 0.170) without detection of unimolecular solved polymers or bigger aggregates (Figure 2C). Interestingly, dissolving only the polymer without siRNA in an aqueous buffer nearly led to the same result (53.4 nm; Pdl 0.190), indicating that the polymer, contrary to general models, already self-assembles into higher-ordered structures even without interaction with the oligonucleotide. This behavior is most likely driven by the  $\beta$ -sheets of pCys(SO<sub>2</sub>Et), which already proved to have strong influence and guidance effects on self-assembly.<sup>[34,36]</sup> Comparison to equal polymeric structures with varying chain lengths of pCys(SO<sub>2</sub>Et) and pLys that are summarized in Table S1, Supporting Information (analytics shown in Figures S6 and S7, Supporting Information), provided interesting insights into the predetermining impact of the polymeric solution properties on the PIC micelle structure. Another triblock copolymer (P2) with comparable or slightly increased block lengths of  $X_{n,p\text{Cys}} = X_{n,p\text{Lys}} = 11$  shows equal aggregation behavior, presenting monomodal and narrow distributed PIC micelles and polymer aggregates as determined by DLS (Figure S8, Supporting Information). By increasing the pLys block to  $X_{n,p\text{Lys}} = 18$  while keep-

ing the size of the other segments (P3), smaller species appeared in the polymeric solution, likely formed by an increased solubility mediated by the more dominant cationic block. However, this effect is counteracted by interaction with the siRNA, also leading to monomodal PIC micelles, which supports the theory of aggregating pseudo-amphiphilic structures derived from charge-neutralization.<sup>[52]</sup> A more drastic influence can be observed by growth of the pCys(SO<sub>2</sub>Et) segment to  $X_{n,p\text{Cys}} = 15$  (P4), resulting in multimodal size distribution with large aggregation products in the polymeric as well as the PIC micelle solution. Further increasing of this block to  $X_{n,p\text{Cys}} = 22$  (P5) only presents huge aggregates in DLS, indicating a complete loss of micellar ordered structures and pointing out the strong influence of the  $\beta$ -sheet forming pCys(SO<sub>2</sub>Et). Thus, PIC micelle structure can be controlled by adjusting the block lengths of pCys(SO<sub>2</sub>Et) and pLys that leads to desired preaggregation of the polymer in aqueous solution. However, as this differs from descriptions in literature, it has to be pointed out, that this behavior is most likely driven by the enormous guiding effect of pCys(SO<sub>2</sub>Et) and therefore only applicable in this specific case.

To investigate and confirm the cross-linking step, the aqueous solution of PIC micelles was lyophilized after cross-linking and redissolved in HFIP to measure GPC (Figure 2D). As expected, the green curve clearly shows free polymers and even smaller species, probably free siRNA or cross-linker molecules. However,

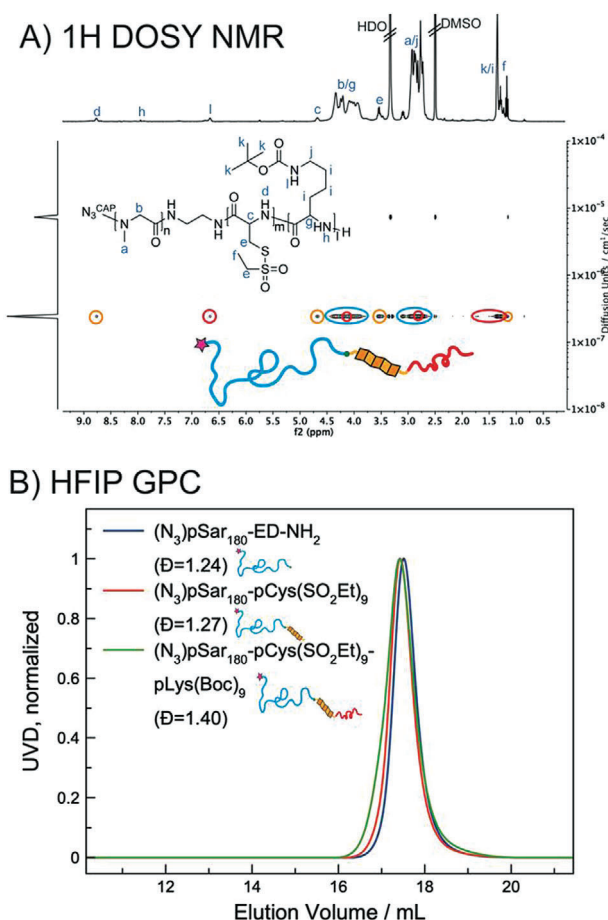


**Figure 1.** Characterization of  $(N_3)pSar$ - $b$ - $pCys(SO_2Et)$ - $b$ - $pLys(Boc)$  ABC-triblock copolymer by A)  $^1H$  DOSY NMR in DMSO and B) HFIP GPC confirming structural integrity, chain growth, and monomodal size-distribution/absence of homo- and diblock polymer.

a larger species is detected at lower elution volumes, giving a strong indication for a functional cross-linking step, resulting in intrinsic stabilized structures by covalent disulfides and preventing polymeric disintegration from the PIC micelle. To remove residual impurities from the PIC micelle solution, that might cause undesired side effects upon application, purification by spinfiltration was applied, utilizing a 100 kDa filter membrane. While PIC micelles are too large to migrate through the filter membrane, they remain in the filter reservoir during centrifugation, whereas smaller species are separated by dilution with aqueous buffer being filtrated, well displayed by the red curve. As a result, the PIC micelles show stability against dilution in aqueous buffer and even in HFIP, testifying a cross-linked structure. To prove and investigate siRNA content of the PIC micelles after purification, dye-labeled siRNA was incorporated for quantification by comparing absorbance to a calibration curve from stock solutions. Pictured in Figure 2E, the content of siRNA after purification was determined for two different siRNAs labeled with Atto488- or AlexaFluor647-dyes (AF647), respectively. Quantification of the contents resulted in a deviation below 5%, suggesting that the dyes do not influence siRNA loading. Excluding an influence of the siRNA itself, content for samples with unlabeled

siRNAs was assessed by comparison to equally processed batches with siRNA-AF647.

An siRNA release study by agarose gel electrophoresis indicated conceptual integrity (Figure S9, Supporting Information). Loaded and purified PIC micelles have been incubated with different glutathione (GSH) levels to mimic extra- (10  $\mu$ M) and intracellular (10 mM) reductive conditions.<sup>[34]</sup> Release could be observed upon addition of varying amounts of dextran sulfate sodium salt, which substitutes the siRNA in the PICs. Without GSH, release could only be detected at high amounts of dextran (5  $\mu$ g), while 10 mM GSH incubation led to significant siRNA release already at 1  $\mu$ g of dextran, as observed by a visible band of free siRNA. Extracellular levels of GSH (10  $\mu$ M) only presented minor release of siRNA at 1  $\mu$ g dextran, indicating higher structural integrity compared to intracellular reductive conditions and further confirm a contribution of disulfide cross-links to siRNA complexation.

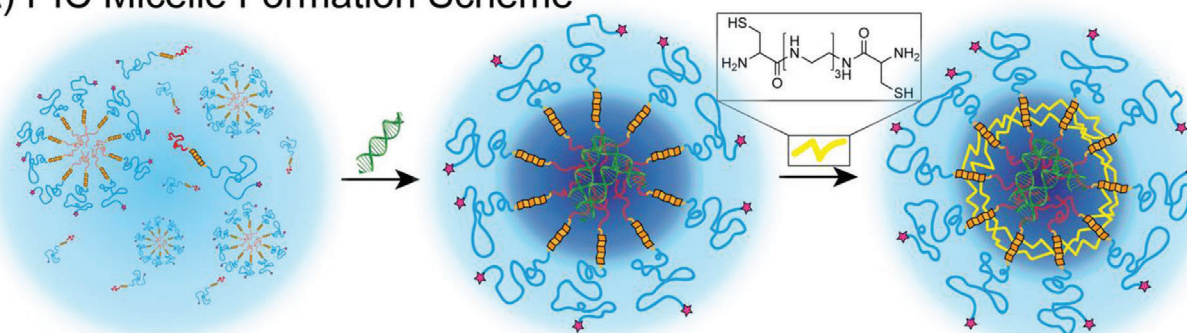
In conclusion, the previous synthesized ABC triblock copolymer  $pSar$ - $b$ - $pCys(SO_2Et)$ - $b$ - $pLys$  could be utilized to generate core cross-linked PIC micelles with good size distribution, stability against aqueous dilution and strong organic solvents, purified from free polymer or other impurities, containing determinable amounts of encapsulated siRNA, and presenting an increased liberation of siRNA at intracellular reductive conditions.

### 2.3. Cellular Delivery of siRNA by PIC Micelles

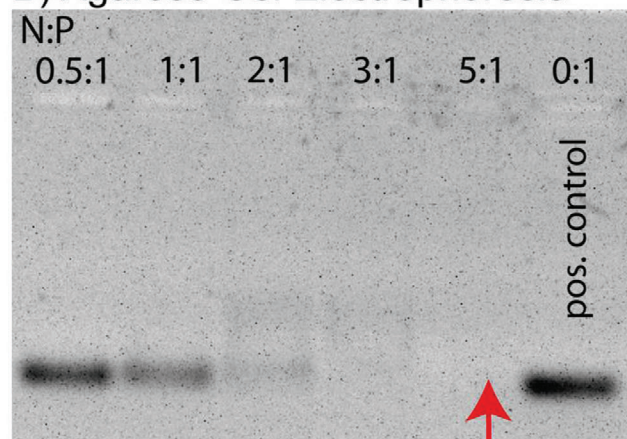
To investigate the capability of the previously characterized PIC micelle to deliver siRNA into cells and therefore mediate gene silencing, several in vitro assays have been performed. The uptake into murine neuroblastoma Neuro2A cells after treatment with siRNA-AF647 containing PIC micelles has been determined by flow cytometry and confocal laser scanning microscopy (CLSM). As displayed in Figure 3A, the cell populations show a dose-dependent uptake of PIC micelles represented by an increase of mean fluorescence intensity (MFI) values with increasing siRNA concentrations between 6.25 and 100 nM. Further, a shift of the total cell populations towards AF647-positive cells can be observed, indicating a good distribution of PIC micelles in the medium and uptake into all cells. As shown in Figure 3B, CLSM confirms the flow cytometry results and illustrated a good PIC micelle distribution (red) inside the cells without extracellular aggregation. For further investigation, siGFP was incorporated into PIC micelles to target an eGFP (enhanced green fluorescent protein)-luciferase fusion reporter gene that is expressed by Neuro2A/eGFP-Luc cells. Knockdown of the mRNA transcribed from the fusion reporter gene can be quantified based on eGFP fluorescence as well as luciferase activity. Here, the decreased reporter gene activity was measured by luciferase assay upon siGFP targeting compared to untargeted siCtrl. A slight dose-dependent knockdown of the reporter gene is observed in a dose range from 25 to 400 nM resulting in an increased reduction of luciferase activity (Figure 3C). However, in doses higher than 100 nM, reduced luciferase activity can also be observed for cells treated with the non-targeting siCtrl, indicating an RNAi independent effect on cell viability. Nevertheless, in lower dosages, a specific reduction of up to 20% (100 nM) in comparison to siCtrl can be seen. To investigate the reason for the rather low specific knockdown



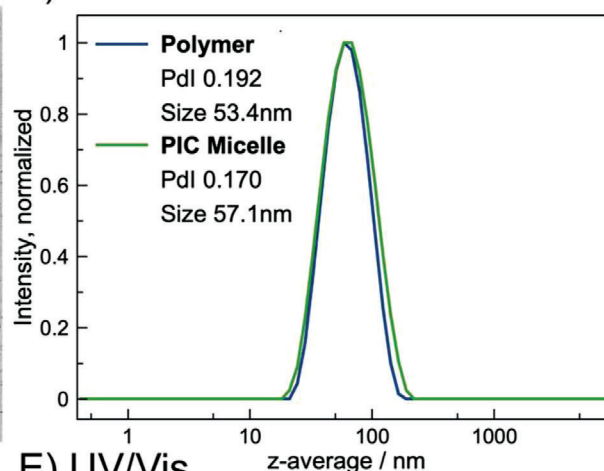
## A) PIC Micelle Formation Scheme



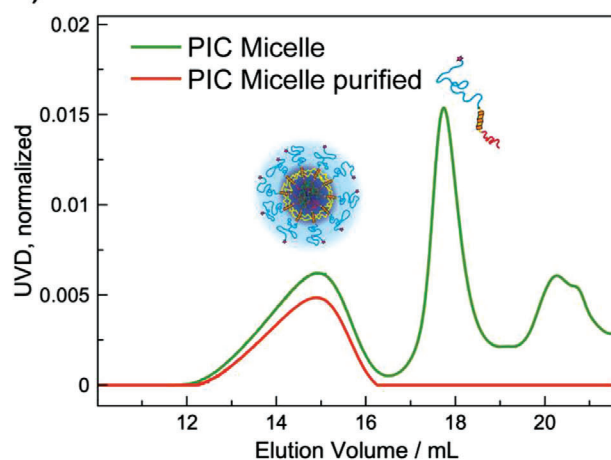
## B) Agarose Gel Electrophoresis



## C) DLS



## D) HFIP GPC



## E) UV/Vis

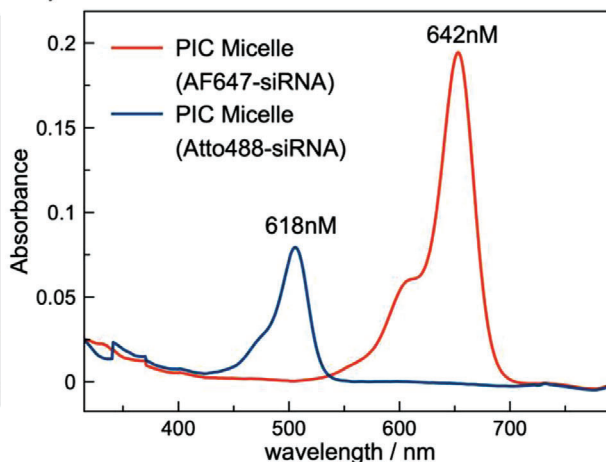
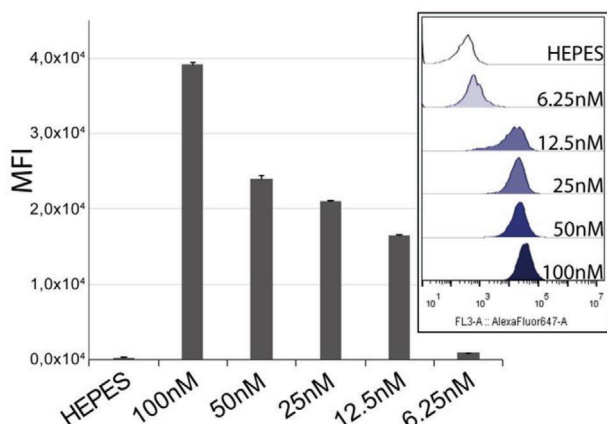


**Figure 2.** A) General scheme of PIC micelle formation by interaction with oligonucleotides and subsequent cross-linking by cTETAc introducing covalent disulfides for intrinsic stability (displayed in bright yellow). B) Agarose gel electrophoresis of ABC-triblock copolymer mixtures with siRNA in 10 mM HEPES buffer at different N/P ratios. C) Dynamic light scattering of PIC micelle in comparison to ABC-triblock copolymer in 10 mM HEPES buffer at 1 mg·mL<sup>-1</sup>. D) Gel permeation chromatography in HFIP of lyophilized PIC micelle solution before and after purification with 100 kDa spinfiltration. E) Determination and quantification of labeled siRNA (Atto488 and AF647) by UV/Vis absorbance.

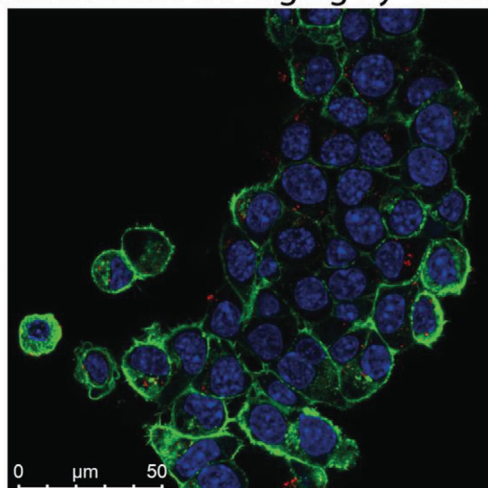
efficiency, chloroquine, a lysosomotropic agent, was added during the transfection, to enforce the endosomal escape.<sup>[45]</sup> With this approach, the specific knockdown efficiency could be significantly increased up to  $\approx 50\%$  (200 nM) but still showing toxicity-mediated effects at higher doses (Figure S10, Supporting Infor-

mation). A possible reason for the dose-dependent toxicity could be that the cells run out of redox-equivalents due to the high amount of disulfides coming with a high load of PIC micelles. An MTT assay was performed to investigate cellular metabolic activity based on redox-equivalents, confirming a significant

### A) Flowcytometric Uptake Analysis



### B) Internalization Imaging by CLSM



### C) eGFP-Luciferase Gene Silencing Efficiency

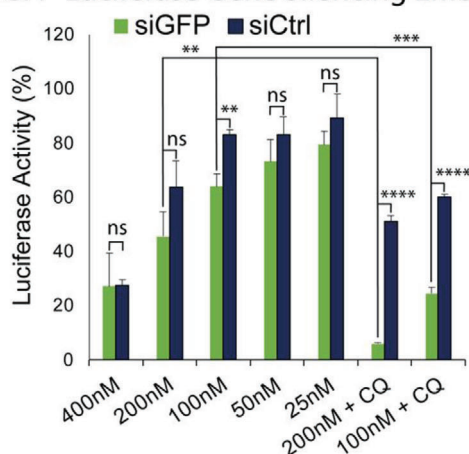


**Figure 3.** In vitro assays in Neuro2A cells using PIC micelles for siRNA delivery: A) Cellular binding and uptake after 4 h incubation with siRNA-AF647 at different concentrations detected by flow cytometry. B) Superimposed CLSM image combining nuclei staining (blue), F-actin staining (green), and PIC micelles containing siRNA-AF647 (red) after 100 nM siRNA treatment for 24 h. Nuclei are stained with DAPI (blue) and the actin skeleton with rhodamine-phalloidin (green). C) eGFP-luciferase gene

reduction at the higher doses (Figure S11, Supporting Information). The in vitro results obtained with Neuro2A cells could also be confirmed with human cervix carcinoma KB cells (Figures S12–S16, Supporting Information). The cellular uptake is observed to be significantly higher in this cell line as determined by flow cytometry (Figure S12, Supporting Information) and CLSM (Figure S13). Also in KB cells, transfections at higher concentrations lead to unspecific reduction of luciferase activity (Figure S14, Supporting Information) and chloroquine treatments identified the endosomal escape as a major hurdle for specific gene knockdown (Figure S15, Supporting Information). MTT assays showed a dose-dependent reduction of metabolic activity (Figure S16, Supporting Information), which eventually could be associated with the high disulfide loading by PIC micelles.

## 3. Conclusion

This work presents the synthesis and characterization of a new ABC-type triblock copoly(ester)ide constructed as combination of a shielding pSar block A, a cross-linkable pCys(SO<sub>2</sub>Et) block B, and a polycationic pLys block C. Most likely caused by the strong guiding effect of the  $\beta$ -sheet forming pCys(SO<sub>2</sub>Et), a preaggregation behavior of the polymer in solution was observed, determining the later structure of the PIC micelle formed by interaction with siRNA. A strong correlation could be derived between the block lengths of the core-forming blocks B and C and the preaggregation behavior. The introduction of cross-links into the loaded PIC micelles supported intrinsic stability and resistance against dilution even in strong organic solvents, which enabled a purification step with an aqueous buffer to remove undesired impurities. Purified PIC micelles showed a dose-dependent siRNA delivery potential into Neuro2A and KB cells but suffered from dissatisfying knockdown efficiency, mainly caused by a low endosomal escape as indicated by the use of chloroquine. Therefore, future development will focus on using ligands, incorporation of endosomolytic moieties and functional cross-linkers to enhance endosomal escape to improve the intracellular delivery of nucleic acids.

## 4. Experimental Section

**Materials and Methods:** Generally, chemicals and materials were purchased from Sigma Aldrich and used as obtained, unless stated otherwise. *N,N*-Dimethylformamide (DMF) (99.8%, extra dry over molecular sieve) was bought from ACROS ORGANICS. DMF was handled under light exclusion and purified by multiple freeze-pump-thaw cycles prior to use. Evaluation of polymerization progress was performed by attenuated total reflectance Fourier transformed infrared (ATR-FTIR) spectroscopy, correlating progress to integrals of NCA-associated IR bands at 1853 and

knockdown in Neuro2A/eGFP-Luc cells is measured by luciferase assay after 4 h incubation with PIC micelles containing siGFP at different concentrations followed by 4 h incubation with medium  $\pm$  chloroquine (CQ, 0.1 mM) and further 44 h post-incubation with fresh medium. Unspecific reduction of luciferase activity is determined by treatment with analog PIC micelles containing siCtrl (mean  $\pm$  sd,  $n = 3$ ). The statistical significance is determined by unpaired *t*-test (two-tail analysis); ns, not significant; \*\* $p \leq 0.01$ , \*\*\* $p \leq 0.001$ , \*\*\*\* $p \leq 0.0001$ .





a total volume of 20  $\mu\text{L}$ . 4  $\mu\text{L}$  of 6x loading dye were added, the samples were pipetted into the gel pockets and electrophoresis was proceeded at 120 V/200 mA for  $\approx 30$  min.

For investigation of siRNA release, 3  $\mu\text{L}$  of purified PIC micelles (3.1  $\mu\text{M}$  siRNA) in 10 mM HEPES buffer have been incubated at different glutathione concentrations (0, 10  $\mu\text{M}$ , 10 mM) at 37  $^{\circ}\text{C}$  for 24 h. Different amounts of dextran sulfate sodium salts (0, 0.1  $\mu\text{g}$ , 0.5  $\mu\text{g}$ , 1  $\mu\text{g}$ , 5  $\mu\text{g}$ ) have been added by stock solutions with 10 mM HEPES buffer, sample volume was filled to 20  $\mu\text{L}$  with 10 mM HEPES buffer and left for incubation for 1 h. 4  $\mu\text{L}$  of 6x loading dye were added, the samples were pipetted into the gel pockets and electrophoresis was proceeded at 120 V/200 mA for  $\approx 30$  min.

**PIC Micelle Preparation:** The triblock copolymer ( $\text{N}_3$ )pSar-b-pCys( $\text{SO}_2\text{Et}$ )-b-pLys was dissolved at 1  $\text{mg}\cdot\text{mL}^{-1}$  in 10 mM HEPES buffer. 100  $\mu\text{L}$  of 5  $\mu\text{M}$  stock solution of the respective siRNA (labeled with AF647/Atto488, targeted or control) were added to 174  $\mu\text{L}$  of the polymer solution, to obtain an N/P ratio of 5 as determined by agarose gel electrophoresis, and vortex a few seconds for good mixing. The sample was left for complexation for 1 h, subsequently 57.3  $\mu\text{L}$  (1.5 eq calculated on Cys( $\text{SO}_2\text{Et}$ ) repeat units) of a cTETAc stock solution (1  $\text{mg}\cdot\text{mL}^{-1}$  in 10 mM HEPES buffer) were added followed by vortexing for a few seconds. The sample was left for cross-linking for another hour and then diluted to 500  $\mu\text{L}$  for better handling. The PIC micelle solution was transferred into a 2 mL Amicon Centrifuge Spinfilter (MWCO 100 kDa) and washed by multiple cycles of centrifugation (3 min, 20  $^{\circ}\text{C}$ , 3000 rpm) and subsequent addition of 10 mM HEPES buffer (total volume of buffer used for washing  $\approx 10$  mL). In the end, the solution was concentrated to  $\approx 300$   $\mu\text{L}$  and removed from the filter, the filter was washed with  $\approx 200$   $\mu\text{L}$  HEPES buffer to obtain 500  $\mu\text{L}$  of PIC micelle solution.

**Cell Culture:** The adherent human cervix carcinoma cell line KB (DSMZ ACC136, Hela subline) and neuroblastoma cell line Neuro2A (ATCC CCL-131) was cultured in Dulbecco's Modified Eagle Medium (DMEM)-low glucose (1  $\text{g}\cdot\text{L}^{-1}$  glucose) supplemented with 10% FBS, 4 mM L-glutamine, 100  $\text{U}\cdot\text{mL}^{-1}$  penicillin and 100  $\mu\text{g}\cdot\text{mL}^{-1}$  streptomycin. The KB/eGFP-Luc and Neuro2A/eGFP-Luc cells stably transfected with the eGFP-Luc (enhanced green fluorescent protein/luciferase) fusion gene were also grown in the supplemented DMEM-low glucose. All cells were incubated at 37  $^{\circ}\text{C}$  in a humidified atmosphere containing 5%  $\text{CO}_2$  and relative humidity of 95%.

**In Vitro Assay for Cellular Binding and Uptake:** PIC micelles were prepared with siRNA-AF647 as described above. To study the cellular binding and uptake efficiency KB or Neuro2A cells were seeded in 96-well plates at a density of  $1 \times 10^4$  cells per well 24 h before the experiment. Thereafter, the medium was carefully aspirated, and the cell treatment was carried out with 80  $\mu\text{L}$  of fresh complete medium and 20  $\mu\text{L}$  of PIC micelle solution in 10 mM HEPES buffer (pH 7.4) to get varying concentrations of encapsulated siRNA (100, 50, 25, 12.5 and 6.25 nM). After 4 h incubation at 37  $^{\circ}\text{C}$ , the treatment medium was discarded, and the cells were washed two times with 300  $\mu\text{L}$  of cold PBS followed by cell harvesting with trypsin/EDTA and centrifugation. The cell pellets were then resuspended in 100  $\mu\text{L}$  cold PBS containing 10% FBS and DAPI (1  $\mu\text{g}\cdot\text{mL}^{-1}$ ). The cell binding and uptake were recorded for 2000 viable cells in triplicates. The threshold level was set based on the background fluorescence of HEPES-treated control cells.

**In Vitro Assay for Gene Knockdown Efficiency:** PIC micelles have been prepared as described above with siRNA targeting GFP (siGFP) mRNA or non-targeting siRNA (siCtrl) as control. The determination of siRNA concentration was made by comparison with batches with labeled siRNA treated the same way in parallel. The gene silencing activity of PIC micelles was determined in KB/eGFP-Luc or Neuro2A/eGFP-Luc cells expressing an eGFP-luciferase fusion reporter gene. In these cells, a specific knockdown of eGFP leads to simultaneous silencing of luciferase. The cells were seeded at  $5 \times 10^3$  cells per well in a 96-well tissue culture plate 24 h prior to transfection. The medium of each well was replaced by 80  $\mu\text{L}$  fresh medium. After 30 min, 20  $\mu\text{L}$  of PIC micelle solution in 10 mM HEPES buffer (pH 7.4) of encapsulated siCtrl or siGFP were added to their respective wells to generate different siRNA concentrations (400, 200, 100, 50, 25 nM). The cell transfection was performed in triplicates with an incubation time of 4 h. The PIC micelle-containing medium was then removed

and the cells were cultured with fresh medium  $\pm$  chloroquine (0.1 mM) for another 4 h followed by additional 44 h incubation in fresh complete medium. Afterward, the medium of each well was exchanged by 100  $\mu\text{L}$  of lysis reagent (Promega, Mannheim, Germany), and the cells were incubated for 45 min at room temperature. The gene silencing activity was measured by determining the luciferase activity of 35  $\mu\text{L}$  cell lysate by adding luciferin solution (10 mM luciferin and 29.4 mM glycylglycine) mixed 1:20 with LAR buffer (20 mM glycylglycine, 1 mM  $\text{MgCl}_2$ , 0.1 mM EDTA, 3.3 mM DTT, 0.5 mM ATP, 0.27 mM Coenzyme A, pH 8–8.5). The luciferase activity was determined as relative light units (RLU) per well which was normalized as percentage of HEPES-treated control cells and presented as means of three independent experiments  $\pm$  sd.

**Cell Viability Assay:** The metabolic activity was evaluated via 3-(4,5-dimethylthiazol-2-yl)-2,5-diphenyltetrazolium bromide (MTT) assay. Briefly, KB or Neuro2A cells ( $5 \times 10^3$  cells per well) were seeded in a 96-well tissue culture plate. After 24 h, the medium was refreshed with 80  $\mu\text{L}$  of complete medium 30 min before transfection with 20  $\mu\text{L}$  of PIC micelle solution in 10 mM HEPES buffer (pH 7.4) containing siCtrl for a range of concentrations of 200, 100, 50, 25, and 12.5 nM. After 48 h exposure, 10  $\mu\text{L}$  of MTT (5  $\text{mg}\cdot\text{mL}^{-1}$ ) was added to each well and the cells were incubated at 37  $^{\circ}\text{C}$  for 2 h. Next, the supernatant was removed, and the cells were frozen at  $-80$   $^{\circ}\text{C}$  for 60 min. The violet crystals were subsequently dissolved in DMSO (100  $\mu\text{L}$  per well), and the plate was kept for 30 min at 37  $^{\circ}\text{C}$  under gentle shaking. The absorption was measured at 590 nm. The cell viability was normalized as percentage of HEPES-treated control cells and presented as means of three independent experiments  $\pm$  sd.

**Confocal Laser Scanning Microscopy (CLSM):** KB or Neuro2A cells ( $2 \times 10^4$  cells per well) were seeded on ibidi  $\mu$ -slide 8-well chamber slides (ibidi GmbH, Martinsried, Germany). On the following day, 50  $\mu\text{L}$  of PIC micelle solution in 10 mM HEPES buffer (pH 7.4) for 100, 50, or 25 nM of siRNA-AF647 was added together with 250  $\mu\text{L}$  fresh medium and the cells were incubated for 24 h at 37  $^{\circ}\text{C}$ . Next, the cells were washed twice with PBS and subsequently incubated with 4% paraformaldehyde (PFA) for 30 min at room temperature. After one more washing step with PBS, the cells were treated with rhodamine-phalloidin (1  $\mu\text{g}\cdot\text{mL}^{-1}$ ) for staining of F-actin, and DAPI (2  $\mu\text{g}\cdot\text{mL}^{-1}$ ) for staining of nuclei under light protected condition for 60 min at room temperature. Afterward, the staining solutions were removed, cells were washed with PBS, and finally supplemented with 300  $\mu\text{L}$  PBS before measurement.

**Statistical Analysis:** The statistical analysis of the results (mean  $\pm$  sd,  $n = 3$ ) was evaluated by two-tailed  $t$ -test (unpaired). Significance levels were defined as ns = not significant,  $**p \leq 0.01$ ,  $***p \leq 0.001$ ,  $****p \leq 0.0001$ .

## Supporting Information

Supporting Information is available from the Wiley Online Library or from the author.

## Acknowledgements

M.Y. appreciates receiving a DAAD fellowship. M.B. and Y.N. have received financial support for this work by the Sino-German cooperation project (GZ1512). M.B. and E.W. would like to acknowledge financial support by the German Research Foundation (DFG) within the Collaborative Research Centers and DFG SFB1066-2/-3 Project B12 and B5 and SFB1032 B4 (E.W.).

## Conflict of Interest

The authors declare no conflict of interest.

## Data Availability Statement

The data that support the findings of this study are available from the corresponding author upon reasonable request.

## Keywords

cross-linking, gene silencing, polyion complex micelles, polypept(o)ides, self-assembly, siRNA delivery

Received: October 20, 2021

Revised: December 14, 2021

Published online: January 17, 2022

- [1] Y. Dong, D. J. Siegwart, D. G. Anderson, *Adv. Drug Delivery Rev.* **2019**, 144, 133.
- [2] A. Harada, K. Kataoka, *Macromolecules* **1995**, 28, 5294.
- [3] A. V. Kabanov, T. K. Bronich, V. A. Kabanov, K. Yu, A. Eisenberg, *Macromolecules* **1996**, 29, 6797.
- [4] A. V. Kabanov, S. V. Vinogradov, Y. G. Suzdaltseva, V. Y. Alakhov, *Bioconjugate Chem.* **1995**, 6, 639.
- [5] Y. Lee, K. Kataoka, *Soft Matter* **2009**, 5, 3810.
- [6] N. Nakamura, Y. Mochida, K. Toh, S. Fukushima, H. Cabral, Y. Anraku, *Polymers* **2020**, 13, 5.
- [7] K. A. Whitehead, R. Langer, D. G. Anderson, *Nat. Rev. Drug Discovery* **2009**, 8, 129.
- [8] M. Talelli, M. Barz, C. J. F. Rijcken, F. Kiessling, W. E. Hennink, T. Lammers, *Nano Today* **2015**, 10, 93.
- [9] S. Reinhard, E. Wagner, *Macromol. Biosci.* **2017**, 17, 1600152.
- [10] S. Uchida, H. Kinoh, T. Ishii, A. Matsui, T. A. Tockary, K. M. Takeda, H. Uchida, K. Osada, K. Itaka, K. Kataoka, *Biomaterials* **2016**, 82, 221.
- [11] G. Creusat, A.-S. Rinaldi, E. Weiss, R. Elbaghdadi, J.-S. Remy, R. Mulherker, G. Zuber, *Bioconjugate Chem.* **2010**, 21, 994.
- [12] P. Heller, D. Hobernik, U. Lächelt, M. Schinnerer, B. Weber, M. Schmidt, E. Wagner, M. Bros, M. Barz, *J. Controlled Release* **2017**, 258, 146.
- [13] R. J. Christie, K. Miyata, Y. Matsumoto, T. Nomoto, D. Menasco, T. C. Lai, M. Pennisi, K. Osada, S. Fukushima, N. Nishiyama, Y. Yamasaki, K. Kataoka, *Biomacromolecules* **2011**, 12, 3174.
- [14] H. Iatrou, K. Dimas, M. Gkikas, C. Tsimblouli, S. Sofianopoulou, *Macromol. Biosci.* **2014**, 14, 1222.
- [15] E. Hara, M. Ueda, C. J. Kim, A. Makino, I. Hara, E. Ozeki, S. Kimura, *J. Pept. Sci.* **2014**, 20, 570.
- [16] N. Ritt, S. Berger, E. Wagner, R. Zentel, *ACS Appl. Polym. Mater.* **2020**, 2, 5469.
- [17] U. Nayanathara, S. S. Keraniyan, G. K. Such, *Macromol. Rapid Commun.* **2020**, 41, 2000298.
- [18] B. S. Kim, H. J. Kim, S. Osawa, K. Hayashi, K. Toh, M. Naito, H. S. Min, Y. Yi, I. C. Kwon, K. Kataoka, K. Miyata, *ACS Biomater. Sci. Eng.* **2019**, 5, 5770.
- [19] K. Klinker, M. Barz, *Macromol. Rapid Commun.* **2015**, 36, 1943.
- [20] A. Birke, D. Huesmann, A. Kelsch, M. Weilbacher, J. Xie, M. Bros, T. Bopp, C. Becker, K. Landfester, M. Barz, *Biomacromolecules* **2014**, 15, 548.
- [21] H. R. Kricheldorf, *Angew. Chem., Int. Ed.* **2006**, 45, 5752.
- [22] A. Birke, J. Ling, M. Barz, *Prog. Polym. Sci.* **2018**, 81, 163.
- [23] T. J. Deming, *Nature* **1997**, 390, 386.
- [24] T. J. Deming, in *Peptide Hybrid Polymers*, Springer-Verlag, Berlin, **2006**, pp. 1–18.
- [25] B. Weber, A. Birke, K. Fischer, M. Schmidt, M. Barz, *Macromolecules* **2018**, 51, 2653.
- [26] P. H. Maurer, D. Subrahmanyam, E. Katchalski, E. R. Blout, *J. Immunol.* **1959**, 83, 193.
- [27] I. Negwer, A. Best, M. Schinnerer, O. Schäfer, L. Capelo, M. Wagner, M. Schmidt, V. Mailänder, M. Helm, M. Barz, H.-J. Butt, K. Koynov, *Nat. Commun.* **2018**, 9, 5306.
- [28] I. Alberg, S. Kramer, M. Schinnerer, Q. Hu, C. Seidl, C. Leps, N. Drude, D. Möckel, C. Rijcken, T. Lammers, M. Diken, M. Maskos, S. Morsbach, K. Landfester, S. Tenzer, M. Barz, R. Zentel, *Small* **2020**, 16, 1907574.
- [29] S. S. Nogueira, A. Schlegel, K. Maxeiner, B. Weber, M. Barz, M. A. Schroer, C. E. Blanchet, D. I. Svergun, S. Ramishetti, D. Peer, P. Langguth, U. Sahin, H. Haas, *ACS Appl. Nano Mater.* **2020**, 3, 10634.
- [30] S. Bleher, J. Buck, C. Muhl, S. Sieber, S. Barnert, D. Witzigmann, J. Huwyler, M. Barz, R. Süß, *Small* **2019**, 15, 1904716.
- [31] K. Son, M. Ueda, K. Taguchi, T. Maruyama, S. Takeoka, Y. Ito, *J. Controlled Release* **2020**, 322, 209.
- [32] O. Schäfer, D. Huesmann, M. Barz, *Macromolecules* **2016**, 49, 8146.
- [33] O. Schäfer, K. Klinker, L. Braun, D. Huesmann, J. Schultze, K. Koynov, M. Barz, *ACS Macro Lett.* **2017**, 6, 1140.
- [34] K. Klinker, O. Schäfer, D. Huesmann, T. Bauer, L. Capelôa, L. Braun, N. Stergiou, M. Schinnerer, A. Dirisala, K. Miyata, K. Osada, H. Cabral, K. Kataoka, M. Barz, *Angew. Chem., Int. Ed.* **2017**, 56, 9608.
- [35] T. A. Bauer, C. Muhl, D. Schollmeyer, M. Barz, *Macromol. Rapid Commun.* **2021**, 42, 2000470.
- [36] T. A. Bauer, J. Imschweiler, C. Muhl, B. Weber, M. Barz, *Biomacromolecules* **2021**, 22, 2171.
- [37] B. Olsen, R. Segalman, *Mater. Sci. Eng., R* **2008**, 62, 37.
- [38] A. Carlsen, S. Lecommandoux, *Curr. Opin. Colloid Interface Sci.* **2009**, 14, 329.
- [39] E. Ramsay, J. Hadgraft, J. Birchall, M. Gumbleton, *Int. J. Pharm.* **2000**, 210, 97.
- [40] S. Kudo, Y. Nagasaki, *Macromol. Rapid Commun.* **2015**, 36, 1916.
- [41] Y. Zhou, S. Han, Z. Liang, M. Zhao, G. Liu, J. Wu, *J. Mater. Chem. B* **2020**, 8, 5564.
- [42] K. Hayashi, H. Chaya, S. Fukushima, S. Watanabe, H. Takemoto, K. Osada, N. Nishiyama, K. Miyata, K. Kataoka, *Macromol. Rapid Commun.* **2016**, 37, 486.
- [43] H. J. Kim, A. Kim, K. Miyata, K. Kataoka, *Adv. Drug Delivery Rev.* **2016**, 104, 61.
- [44] A. I. S. Van Den Berg, C.-O. Yun, R. M. Schiffelers, W. E. Hennink, *J. Controlled Release* **2021**, 331, 121.
- [45] U. Lächelt, E. Wagner, *Chem. Rev.* **2015**, 115, 11043.
- [46] J. Sana, P. Faltejskova, M. Svoboda, O. Slaby, *J. Transl. Med.* **2012**, 10, 103.
- [47] T. M. Rana, *Nat. Rev. Mol. Cell Biol.* **2007**, 8, 23.
- [48] S. R. Eddy, *Nat. Rev. Genet.* **2001**, 2, 919.
- [49] D. Castanotto, J. J. Rossi, *Nature* **2009**, 457, 426.
- [50] O. Schäfer, D. Huesmann, C. Muhl, M. Barz, *Chem. – A Eur. J.* **2016**, 22, 18085.
- [51] E. Tsuchida, Y. Osada, K. Abe, *Die Makromol. Chemie* **1974**, 175, 583.
- [52] M.-H. Dufresne, J.-C. Leroux, *Pharm. Res.* **2004**, 21, 160.
- [53] H. E. Gottlieb, V. Kotlyar, A. Nudelman, *J. Org. Chem.* **1997**, 62, 7512.